High-frequency waves in bismuth in the cyclotron-resonance region

M. R. Trunin and V. S. Édel'man

Institute of Solid State Physics, USSR Academy of Sciences; Institute of Physics Problems, USSR Academy of Sciences; Institute for Microelectronics Technology and Ultrapure Materials, USSR Academy of Sciences

(Submitted 9 July 1986)
Zh. Eksp. Teor. Fiz. **92**, 988–1000 (March 1987)

The cyclotron-wave spectrum in bismuth is calculated in the range $0 \leqslant kR \leqslant 10$ (k is the wave number and R is the orbit radius in the magnetic field.) The locations of the turning points in the wave spectrum are compared with the experimentally observed impedance singularites. The calculation agrees with experiment to within 0.1% in the case of cyclotron waves near hole resonances. In magnetic fields close to the light-electron cyclotron resonances, another structure, not yet fully explained, is observed in addition to the singularities obtained by calculation.

INTRODUCTION

Various weakly damped waves can propagate in bismuth, such as fast magnetosonic and Alfven waves, cyclotron waves, or waves due to the anisotropy of the medium (see the references in Édelman's reviews[1,2]). These waves exist if the sample is placed in a magnetic field H such that the characteristic cyclotron frequencies Ω are comparable with or much higher than the frequencies ω of the applied electric field. The oscillations observed in most cases are long-wave, such that the sample thickness spans an integer number of half-waves as the field H is varied and the surface impedance of the metal oscillates resonantly. However, singular points in the wave spectrum, which correspond to one of the conditions $k = 0$ or $dk/d\omega = \infty$, can lead to singularities of the impedance of a semi-infinite metal. Such points are present in the cyclotron-wave spectrum.

Cyclotron waves are classified in accordance with the value of the parameter kR (R is the Larmor radius) and with the orientation of the electric field $\mathbf{E}$ relative to the external field $\mathbf{H}$. The wave is called ordinary if $\mathbf{E} \| \mathbf{H}$ and extraordinary if $\mathbf{E} \perp \mathbf{H}$. Long waves are excited for $kR < 1$ and short ones for $kR > 1$.

It is known that in metals having spherical Fermi surfaces the dispersion curves $k(\omega)$ of the cyclotron waves begin ($k = 0$)[3] and end ($k \to \infty$)[4] at cyclotron frequencies $\Omega = \omega/n$ (n is an integer). In the intermediate case $kR \gtrsim 1$ the wave spectrum oscillates.[5] The situation in bismuth is made more complicated by the presence of several types of carrier. The value of k can reach zero even outside the cyclotron-resonance field,[6] the wave propagation regions may overlap near the hole and electron resonances,[7] various wave types exist simultaneously in the vicinity of hole resonances,[8–10] etc.

Cyclotron resonances were observed in the long-wave limit $kR \ll 1$ in alkali metals[11] and in bismuth near electron[12–14] and hole[10] resonances. Singularities related to turning points of the dispersion curve can occur in the intermediate region. Accurate identification of these singularities calls for a numerical calculation of the cyclotron-wave spectrum. Spectrum turning points in the plots of the impedance vs the magnetic field have so far been observed only in silver[15] and potassium.[16]

A second-harmonic signal reflected in bismuth from the surface exhibited singularities that were identified in Ref. 7 with turning points of the spectrum of cyclotron waves propagating near high-multiplicity hole resonances. Note that in the linear regime the dependence of the bismuth impedance on the magnetic field is extremely intricate and entangled. Furthermore, the better the sample quality, the more diverse the "fine" structure. One example is cited in Ref. 2, where it is suggested that some of the additional singularities are due to excitation of short-wave cyclotron waves.

The first theoretical investigations of high-frequency waves in bismuth were started by Fal'kovskii[17] two decades ago. Practical cyclotron-wave calculations, which become quite laborious at $qR > 1$, have become feasible only quite recently. A computer algorithm described in Ref. 7 has enabled us to undertake a calculation of the cyclotron-wave spectrum and its comparison with the experimental dependences of bismuth impedance on the magnetic field. The results are described below.

EXPERIMENT

The experimental results discussed below were actually obtained in the course of a study[18] aimed mainly at finding the frequency and temperature dependences of the cyclotron-resonance linewidth; the results described here have not been published previously. Since the experimental procedure was described in detail in Ref. 18, we mention only some details of importance below.

We investigated a Bi single crystal in the form of a disk 18 mm in diameter and 2 mm thick, with the normal to the flat surface aligned with the trigonal axis C_3. The magnetic field was set parallel, to the sample plane to within several minutes of angle, as monitored by the dependence of the cyclotron resonance linewidth on the field inclination. The field orientation relative to the crystallographic axes C_1 (bisector) or C_2 (binary) was determined to ~ 10–$15'$ from the symmetry of the effect.

The quality of the sample was such that at ~ 18 GHz the parameter $\omega\tau$ (τ is the relaxation time) reached ~ 120 for light electrons and ~ 400 for heavy holes. The value of $\omega\tau$ for light electrons decreased with increasing frequency.[18]

Measurments at ~ 10 GHz were made using a strip resonator that ensured a strictly linear polarization of the rf electric field $\mathbf{E}$ on the sample. Cavity or dielectric resonators

 0038-5646/87/030560-08$04.00

were used at higher frequencies. The polarization of **E** was then no longer linear and a mixture of responses corresponding to both **E**||**H** and **E**⊥**H** was recorded. This fact will be taken into account in the subsequent comparison with the calculations.

CALCULATION OF THE WAVE SPECTRUM

The dispersion equation for waves propagating perpendicular to a static magnetic field **H** in an unbounded medium is given by (**H**||z)

$$\begin{vmatrix} \sigma_{yy} & \sigma_{yx} & \sigma_{yz} \\ \sigma_{xy} & \sigma_{xx}-\dfrac{k^2c^2}{4\pi i\omega} & \sigma_{xz} \\ \sigma_{zy} & \sigma_{zx} & \sigma_{zz}-\dfrac{k^2c^2}{4\pi i\omega} \end{vmatrix} = 0. \tag{1}$$

Here ω is the wave frequency, **k**||y is the wave vector (y is the normal to the surface if the body is bounded), and σ_{ik} (**k**, ω, **H**) are the Fourier components of the conductivity.

The electron Fermi surface of bismuth is known to deviate somewhat from an ellipsoid.[2,19] We shall, however, assume it to be an ellipsoid, in view of the integral character of the conductivity tensor components and of the fact that the main contribution to them is made, in the case **E**⊥**H** of principal interest to us, by the electrons near the central cross section, where the deviations from ellipsoidal form are immaterial. According to this model the Fermi surface of bismuth consists of one hole ellipsoid and three electron ellipsoids. In the coordinate frame with principal axes, 1, 2, and 3 the energy of the electrons of one of the ellipsoids is

$$\varepsilon_e = \frac{1}{2m_0}(\alpha_{1e}p_1^2+\alpha_{2e}p_2^2+\alpha_{3e}p_3^2), \tag{2}$$

where α_{ie} and P_i, respectively, are the components of the inverse effective-mass tensor and the momenta of the electrons in terms of the principal axes. The α_{ie} are expressed in terms of the measured (see Ref. 2) cyclotron masses m_i along the axes $i = 1, 2, 3$: $\alpha_{ie} = m_1/m_2m_3$, $\alpha_{2e} = m_2/m_1m_3$, $\alpha_{3e} = m_3/m_1m_2$. The volume of the electron surface is

$$V_e = {}^4/_3\pi(8m_1m_2m_3)^{1/2}\varepsilon_e^{3/2} = 14.66\cdot 10^{-63}\ \text{g}^3\cdot\text{cm}^3/\text{s}^3$$

and hence $2\varepsilon_e = 5{,}74\times 10^{-14}$ erg.

We obtain the energy of the hole ellipsoid of revolution (h), whose axis is parallel to the C_3 axis,[1] from the condition that the volumes of the electron and hole surfaces in bismuth be equal: $\varepsilon_h = 1{,}85\times 10^{-14}$ erg. In the crystal coordinate frame, the hole dispersion law takes the form

$$\varepsilon_h = \frac{1}{2m_0}(\alpha_{1h}p_1^2+\alpha_{2h}p_2^2+\alpha_{3h}p_3^2), \tag{3}$$

where p_1, p_2, and p_3 are the components of the momentum vector along the axes C_1, C_2, and C_3, while the values of α_{ih} are, acording to Ref. 2,

$$\alpha_{1h}=\alpha_{2h}={}^1/_{0{,}064}, \quad \alpha_{3h}={}^1/_{0{,}703}.$$

Let the static magnetic field be applied in the trigonal plane of the crystal. We obtain the spectrum of the high-frequency waves in Bi for two magnetic-field orientations: **H**||C_2 and **H**||C_1.

1. Magnetic field directed along the C_2 axis: **H**||C_2||z, **k**||C_3||y, C_1||x. Rotating the ellipsoid (2), we obtain in the xyz coordinate frame

$$\varepsilon_e = \frac{1}{2m_0}(\alpha_{xx}p_x^2+\alpha_{yy}p_y^2+\alpha_{zz}p_z^2+2\alpha_{xy}p_xp_y), \tag{4}$$

where $\alpha_{xx} = 1{,}89$, $\alpha_{yy} = 89{,}08$, $\alpha_{zz} = 164{,}91$, $\alpha_{xy} = 9{,}88$. We refer to the ellipsoid defined by (4) as ellipsoid a. The energy spectra of the two other electron ellipsoids b and c are obtained by rotating ellipsoid a through $\pm$ 120° around the C_3 axis.

Using the chosen electron and hole dispersion laws (4) and (3), respectively, we can calculate all the components of the conductivity tensor σ_{ik}. This was done in Appendix A of Ref. 7. We write down here only the component with the simplest form, σ_{yy}, for one arbitrary group of carriers:

$$\sigma_{yy} = \frac{\alpha_{yy}N}{(kR)^2}\sum_{n=-\infty}^{\infty}\frac{n^2}{\nu-i(\omega-n\Omega)}\int_0^{\pi/2}d\theta\sin\theta J_n^2(kR\sin\theta), \tag{5}$$

where

$$\begin{gathered} N=(2\varepsilon)^{3/2}me^2/\pi^2\hbar^3\gamma^{1/2}, \quad \Omega=eH/mc, \quad R=(2\varepsilon\alpha_{yy})^{1/2}/\Omega, \\ m=(\alpha_{xx}\alpha_{yy}-\alpha_{xy}^2)^{-1/2}, \\ \gamma=\alpha_{zz}+m^2(2\alpha_{xz}\alpha_{yz}\alpha_{xy}-\alpha_{xz}^2\alpha_{yy}-\alpha_{yz}^2\alpha_{xx}). \end{gathered} \tag{6}$$

Here m, Ω, and R are the carrier cyclotron mass, frequency, and orbit radius, respectively, $\nu = 1/\tau$ is the collision frequency, and J_n is a Bessel function of order n.

The integrals in the expressions for σ_{ik} can be expressed in terms of elementary functions in the limits of weak ($kR \ll 1$) or strong ($kR \gg 1$) spatial dispersion. In the intermediate case ($kR \gtrsim 1$) the conductivity tensor elements can be determined only numerically.

The task of finding the high-frequency-wave spectrum in bismuth reduces to calculation of the components σ_{ik} with allowance for the contributions from all carrier groups, and to solution of the dispersion equation (1). It is easily seen that in the present case **H**||C_2||z, **k**||C_3||y, C_1||x the off-diagonal non-Hall components σ_{ik} are zero:

$$\sigma_{xz}=\sigma_{xz}^{(a)}+\sigma_{xz}^{(b)}+\sigma_{xz}^{(c)}+\sigma_{xz}^{(h)}=0, \quad \sigma_{zx}=\sigma_{yz}=\sigma_{zy}=0.$$

Equation (1) breaks up therefore into two equations:

$$\sigma_{zz}-k^2c^2/4\pi i\omega=0, \tag{7}$$

$$(k^2c^2/4\pi i\omega)\sigma_{yy}-\sigma_{xx}\sigma_{yy}+\sigma_{xy}\sigma_{yx}=0. \tag{8}$$

The ordinary wave is described by Eq. (7). It is purely transverse, and its electric field **E**||z. The extraordinary wave satisfies Eq. (8), is not purely transverse, and is polarized in a plane perpendicular to the magnetic field (**E**⊥z).

We find now the solutions of (7) and (8) in the region of the first and second resonances of the b- and c-electrons. For **H**||C_2, **k**||C_3 we have from (3), (4), and (6)

$$\begin{gathered} m^{(b)}=m^{(c)}, \quad m^{(b)}/m^{(a)}=8.01\cdot 10^{-2}, \quad m^{(b)}/m^{(h)}=4.49\cdot 10^{-2}, \\ R^{(b)}=R^{(c)}, \quad R^{(a)}=12.49R^{(b)}, \quad R^{(h)}=2.26R^{(b)}. \end{gathered} \tag{9}$$

Note that the integrals of the small and large values of kR for different carriers do not always overlap, in view of the large difference between the orbit radii (9). This circumstance must be taken into account in calculations of the resultant component of the tensor σ_{ik}.

We are interested in the special cyclotron-wave-spectrum points that lead to the experimentally observed anomalies of the impedance of bismuth as a function of the external magnetic field.

In the long-wave limit ($kR \ll 1$) these points are dielectric anomalies, viz., singularities corresponding to $k = 0$. They were first observed in Ref. 6 as maxima of the absorption coefficient of Bi (Ref. 6).[2] Assuming that the condition $kR \ll 1$ is met for all carrier groups, the components σ_{ik} can be expanded in powers of $(kR)^2$ and only the first few terms need be retained. Analysis shows that a dielectric anomaly exists in this region of the first and second b-electron cyclotron resonances only for the ordinary wave (7): $k = 0$ for $\theta / \Omega^{(b)} = 0.84$. The dispersion curve of the extraordinary wave tends to hug the cyclotron-resonance line from the direction of the stronger magnetic fields. Equation (8) has then one solution near the first resonance and two solution near the second. The extraordinary wave is known to behave in the same manner for the case of a spherical Fermi surface.[11]

In the short-wave limit $kR \gg 1$, it is the turning points of the wave spectrum which are special. In this case the expressions for the conductivity-tensor elements can be represented as series in powers of $(1/kR)$ (see Appendix B of Ref 7), so that the oscillation period of the functions σ_{ik} (kR) is equal to π, and the oscillation amplitude decreases as kR increases. It is easy to verify that the leading term $\sigma_{xy}\,\sigma_{yx}$ of the left-hand side of expansion (8) is proportional to $(kR)^{-5}$. Therefore if only terms of only lower powers of $(1/kR)$ are retained, the extraordinary-wave dispersion equation breaks up into a pair of equations:

$$\sigma_{yy}=0, \tag{10}$$

$$\sigma_{xx}-k^2c^2/4\pi i\omega=0. \tag{11}$$

Equations (10) and (11) define the propagation of linearly polarized longitudinal and transverse waves. Figure 1 shows the solutions of Eq. (11) for three different frequencies in the absence of collisions ($\Omega\tau \to \infty$). The expansion of σ_{xx} holds through terms $(kR)^{-2}$ inclusive. The values of R and Ω in Fig. 1. pertain to electrons of ellipsoid b. The vertical arrows mark certain limiting point of the spectrum, at which the wave group velocity vanishes. It can be seen that with increase of the alternating-field frequency the spectrum turning points are shifted into magnetic fields corresponding to lower values of $\Omega^{(b)}/\omega$, and that with increase of $kR^{(b)}$ the dispersion curves approach rapidly the cyclotron-resonance lines.

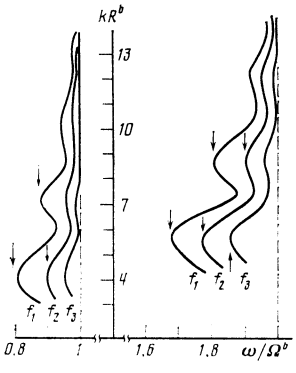

FIG. 1. Numerical solution of Eq. (11) in the regions of the first and second light-electron resonances for three different frequencies $f_1 = 19$, $F_2 = 31, f_3 = 52$ GHz; $\mathbf{H}\|C_2$, $\mathbf{k}\|C_3$, $\Omega\tau \to \infty$.

The asymptotic expansion of the conductivity tensor cannot be used for b-electrons in the intermediate case ($kR^{(b)} \sim 1$). A solution must be sought for the complete equation (8), and the components $\sigma_{ik}^{(b)}$ must be calculated directly from general expressions of type (5), retaining in the sums only a number $n_{\max}$ of terms, such that the result is not changed, at the required accuracy of σ_{ik}, by adding terms of higher order. As to the contribution made to conductivity by the holes and electrons of ellipsoid a, we can state the following. In view of the finite relaxation times of the electrons and holes, it can be easily shown that at $kR^{(b)} \lesssim 2$ inclusion of larger numbers of cyclotron resonances of these carriers in the region considered, $0.7 < \omega/\Omega^{(b)} < 2$, does not alter the values of $\sum_n \sigma_{ik}^{(h)}$ and $\sum_n \sigma_{ik}^{(a)}$ calculated for $n < 10$. At $kr^{(b)} > 2$, according to (9), one can use for the components $\sigma_{ik}^{(h)}$ and $\sigma_{ik}^{(a)}$ asymptotic expressions in the short-wave limit. The extraordinary cyclotron wave spectrum calculated in the interval $0 \leqslant kR^{(b)} \leqslant 10$ will be considered in greater detail later (Fig. 8).

2. Let the magnetic field now be directed along the C_1 axis: $\mathbf{H}\|C_1\|z$, $\mathbf{k}\|C_3\|y$, $C_2\|x$. The hole dispersion law is described as before by expression (3), and for the electrons of ellipsoid a we have

$$\varepsilon_e = \frac{1}{2m_0}\left(\alpha_{xx}p_x^2+\alpha_{yy}p_y^2+\alpha_{zz}p_z^2+2\alpha_{yz}p_yp_z\right), \tag{12}$$

where $\alpha_{xx} = 164.91$, $\alpha_{yy} = 89.08$, $\alpha_{zz} = 1.89$, $\alpha_{yz} = 9.88$. The relations between the cyclotron masses and the radii of the different carrier groups are, according to (3), (6), and (12),

$$m^{(b)}=m^{(c)}, \quad m^{(a)}/m^{(b)}=0.50, \quad m^{(h)}/m^{(b)}=12.94,$$
$$R^{(b)}=R^{(c)}, \quad R^{(a)}=0.50R^{(b)}, \quad R^{(h)}=1.31R^{(b)}.$$

In the case considered with $\mathbf{H}\|C_1$ and $\mathbf{k}\|C_3$ all the elements of the conductivity tensor differ from zero, and to find the wave spectrum we must solve the general dispersion equation (1). Such a calculation (with somewhat different parameters of the carrier dispersion law) was carried out in Ref. 7 for the region of the first two cyclotron resonances of the b-electrons. The use of the asymptotic expressions for the components σ_{ik} in the limiting cases $kR \ll 1$ and $kR \gg 1$ has made it possible to separate the different branches of the spectrum.

At large wavelengths ($kR \ll 1$) the non-Hall off-diagonal components σ_{ik} are small compared with the remaining elements of the conductivity tensor to within terms of order $(kR)^2$, and Eq. (1) breaks up into the system of two equations (7) and (8). The special point of the ordinary-wave spectrum is the dielectric anomaly — the $k = 0$ singularity in the field $\Omega^{(b)}/\omega = 2.36$. The dispersion curve for the extraordinary wave at $kR < 1$ as calculated in Ref. 7 is in error. The correct answer is the following. At $k = 0$ the extraordinary-wave branch coincides with the cyclotron-resonance line; $\Omega^{(b)}/\omega = 0.5$ and $\Omega^{(b)}/\omega = 1$. In addition, a dielectric anomaly exists at $\Omega^{(b)}/\omega = 0.68$, and with increase of kR the branch that starts out in this magnetic field hugs the line of the first cyclotron resonance. These two anomalies were distinctly noted in Ref. 6 (Fig. 11, peaks at fields

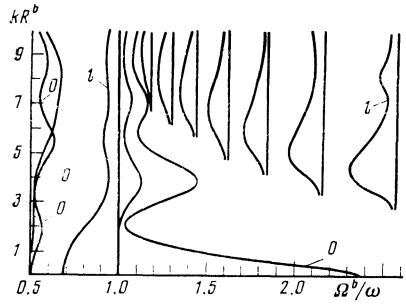

FIG. 2. Bismuth cyclotron-wave spectrum obtained in the region of the first two cyclotron resonances by numerical solution of the dispersion equation (1) $\mathbf{H}\|C_1, \mathbf{k}\|C_3$, $\omega/2\pi = 10.22$ GHz, $\omega\tau \to \infty$.

$H \approx 275$ Oe and $H \approx 950$ Oe; the structure in the field $H \approx 2650$ Oe is due to the second hole cyclotron resonance).

The spectrum of the cyclotron waves in the intervals $0 \leqslant kR^{(b)} \leqslant 10$ and $0.5 \leqslant \Omega^{(b)}/\omega \leqslant 2.6$ is shown in Fig. 2. The letter o marks the ordinary-wave branch (7), and the letter l that of the longitudinal wave, described in the $kR \gg 1$ limit by Eq. (10). The longitudinal waves propagate in the regions of the first electron resonance and of the high-number hole resonances from the direction of the weaker magnetic fields. The unmarked branches near the electron resonances correspond to the extraordinary wave. This spectrum was obtained by numerical solution of the general equation (1), with the first 15 terms of the sum ($n_{max}^{a,b,c,h} = 15$) included in expressions of type (5) for the components σ_{ik}. The error in the calculation of the spectrum is less than 0.1% in terms of $\Omega^{(b)}/\omega$.

The spectrum of the high-frequency waves, shown in Fig. 3, was calculated similarly in the region of the first hole resonances. Let us examine in greater detail the origin of the branches of this spectrum.

Equations (7) and (8) are valid in the limit $kR \ll 1$. In strong magnetic fields $\Omega^{(h)} \gg \omega$, the product of the Hall components of the conductivity is smaller by a factor $(\Omega^{(h)}/\omega)^2$ than the product of the diagonal ones, and Eq. (8) breaks up into (10) and (11). Equation (10) has no roots under conditions of weak spatial dispersion, while the solution of (11) determines the linear spectrum and the polarization of the magnetosonic wave: $\omega/\Omega^{(h)} \sim k$. As the magnetic field decreases, the Hall elements of the conductivity tensor become equal to the diagonal ones, and the magnetosonic-wave spectrum becomes nonlinear. In addition, as follows from (8), there exists one more cyclotron branch of the spectrum, hugging very closely the line of the first hole resonance on the side of the stronger magnetic fields (not shown in Fig. 3). The maximum deviation of this branch from the resonance line, which takes place at $kR^{(h)} = 0.48$, is equal to $\omega/\Omega^{(h)} = 0.993$. Analysis shows that the magnetosonic and cyclotron branches coalesce at this turning point, and with further increases $kR^{(h)}$ they hug the resonance line. Finally, at $kR^{(h)} \approx 0.5$ Eq. (8) acquires a new solution corresponding to a cyclotron wave whose existence region extends to magnetic fields A numerical calculation for the region $kR^{(h)} \gtrsim 1$ shows that the dispersion curve of this wave (which appears to be a continuation of the magnetosonic branch) does not reach the second hole resonance, but instead turns around, oscillates at large $kR^{(h)}$, and approaches the first resonance from the direction of the weaker fields. For $kR^{(h)} > 5$ the spectrum of this wave is well described by Eq. (10) if the asymptotic expression for σ_{yy} (Ref. 7) is used. The ordinary wave (7) is practically merged with the resonance line in the entire region of variation of $kR^{(h)}$.

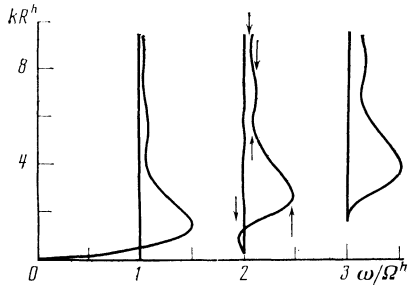

FIG. 3. Bismuth wave spectrum in the region of the first three hole resonances; $\mathbf{H}\|C_1$, $\mathbf{k}\|C_3$, $\omega/2\pi = 10.22$ GHz $\omega\tau \to \infty$. The arrows mark the turning points of the spectrum in the region of the second resonance.

The above picture of the spectrum of the high-frequency waves in the vicinity of the first hole resonance was obtained under the assumption $\Omega\nu \to \infty$. The various branches of this spectrum cannot be separated if damping is taken into account. We note also that, given the carrier dispersion laws (3) and (12), the locations of the turning points of the spectrum in the magnetic field are determiend by only one parameter, viz., the frequency ω of the alternating field. As the frequency rises from the value $\omega/2\pi = 10.22$ GHz, the turning point of the spectrum, located in Fig. 3 at $kR^{(h)} < 5$, shift into the region of weaker magnetic fields. For example, when the frequency ω is increased threefold, the branch located near the second hole resonance on the side of the stronger fields merges with the resonance line. The spectrum of the longitudinal wave (10) is independent of the frequency ω.

COMPARISON WITH EXPERIMENT

If we recognize that the hole Fermi surface is quite close to ellipsoidal,[2,19] it is natural to compare first with experiment the hole cyclotron resonances, for which one can expect good quantitative agreement beforehand.

We begin with the experimental plot of the bismuth impedance at the frequency $\omega/2\pi = 10.22$ GHz at $\mathbf{H}\|C_1$, $\mathbf{k}\|C_3$, $\mathbf{H}\perp\mathbf{E}$ in the region of the second hole resonance, has a well resolved fine structure not distorted by resonances from standing waves (Fig. 4). This plot shows singularities in fields $\Omega^{(h)}/\omega = 0.513$, 0.485, 0.476, 0.471 near the resonance minimum $\Omega^{(h)}/\omega = 0.5$. The amplitudes of these singularities are comparable with or even exceed the signal at the resonance itself. In addition, a deep minimum is present at $\Omega^{(h)}/\omega = 0.408$. All these singularities, which are marked by arrows, are manifestations of the wave-spectrum boundaries indicated in Fig. 3.

The dispersion curves at $\Omega^{(h)}/\omega \approx 0.5$, shown in Fig. 3, were obtained by solving Eq. (1), in which were substituted the conductivity tensor elements calculated from the general equations ($n_{max}^{a,b,c,h} = 15$). Using the asymptotic expressions for the components σ_{ik} it is easy to show that the oscillating curve is accurately described by Eq. (8) at $kR^{(h)} < 1$, and by Eq. (10) at $kR^{(h)} > 4$ for a longitudinal wave. The splended agreement between experiment and theory is achieved without any fitting whatever, using the parameters of the energy

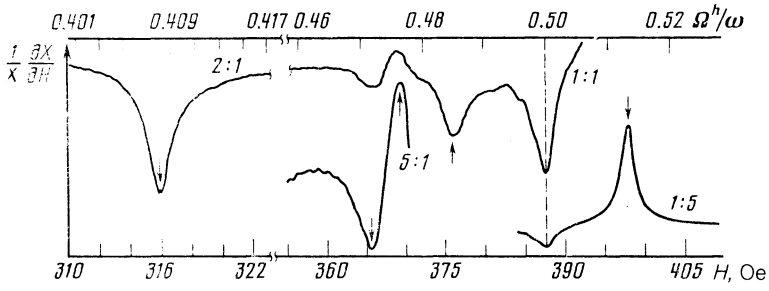

FIG. 4. Surface impedance of bismuth vs. the magnetic field in the region of the second hole resonance. The experimental plot was obtained for $\mathbf{H}\|C_1$, $\mathbf{k}\|C_3$, sample thickness 2 mm, frequency 10.22 GHz, $T = 0.35$ K.

spectra given in Ref. 2 for holes [Eq. (3)] and electrons [Eq. (12)].

This agreement permits certain qualitative conclusions to be drawn concerning the singularities of the impedance, without calculating the latter. First, it is clearly seen that the singularities at $\Omega^{(h)}/\omega = 0.408$ and 0.513, which correspond to turning points that limit the regions in which waves are present in the weaker and stronger magnetic field, respectively, have opposite signs, which is natural. Second, the amplitude of the effect is larger for smaller absolute values of k at the turning point. A similar behavior can be noted also for the singularities $\Omega^{(h)}/\omega = 0.476$ and 0.471. The only exception is the singularity at $\Omega^{(h)}/\omega = 0.485$, but it seems that in this case several singularities located at $kR^{(h)} > 8$ are superimposed.

We consider now the region of the first hole resonance. If $\mathbf{H}\|C_1$, $\mathbf{k}\|C_3$, $\mathbf{E}\perp\mathbf{H}$, weakly damped high-frequency waves with wavelength exceeding the Larmor radius are excited in this range of magnetic fields. In strong fields, $\Omega^{(h)}/\omega > 1$, a single wave is excited, and its spectrum is shown in Fig. 3. Each successive oscillation of this wave changes by unity the total number of half-waves spanned by the sample thickness d, i.e., the periodicity of the oscillations is determined by the condition $n\lambda/2 = d$. The experimental curve coincides with the theoretical under this condition (Fig. 3) all the way to $\Omega^{(h)}/\omega \approx 1$. Figure 5 shows the two minima numbered $n = 260$ and 261 near the first hole resonance. It can also be seen that the amplitude of the oscillations decreases abruptly and approaches the point $\Omega^{(h)}/\omega = 1.007$, which marked by an arrow and is the end point of the spectrum of the extraordinary cyclotron wave. The observed damping of the standing waves in a narrow region near $\Omega^{(h)}/\omega \approx 1$ is of fundamental significant. Indeed, as shown in Ref. 3 and confirmed by experiments on samples of lower quality (see Ref. 1), the hole cyclotron resonance of first order is not manifested in the impedance and in the magnetosonic-wave damping which is proportional in the local limit to $(\omega\tau)^{-1}$. The appearance of a region with strong damping, which is observed only in the better samples, i.e., at larger τ, attests to the presence of a nonlocal interaction. The structure observed in the immediate vicinity of $\Omega^{(h)}/\omega = 1$ is apparently due to "intermixing" of the cyclotron and magnetosonic waves. Starting from the field value at which the spectrum branches cross, we can conclude that observation of nonlocal damping calls for $\omega\tau \gg 1/0.007 \approx 150$. Of all the known experiments, this condition is met only by the experiments described here, in which $\omega\tau \approx 400$–500 for holes. One cannot exclude in principle the possibility of additional wave damping due to small ($< 1\%$, but unknown[19]) deviations of the hole spectrum from a quadratic one. Since, however, the wave spectrum was calculated assuming it cannot be made to accord with the structure of the impedance when the detuning from resonance is $< 1\%$, nor can attempts be made at all to conclude that the hole Fermi surface is not ellipsoidal.

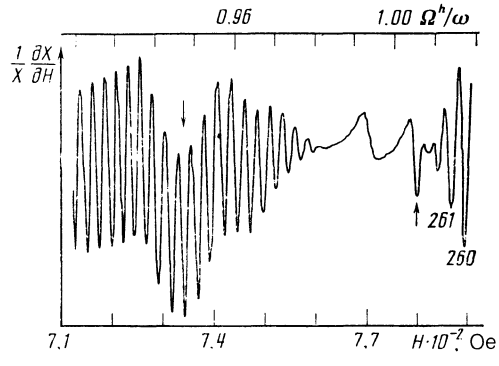

FIG. 5. The same as Fig. 4., but near the first hole cyclotron resonance.

With further deviation from resonance, the dispersion curve acquires, in accordance with the calculation, a turning point at $\Omega^{(h)}/\omega = 0.947$ superposed on the oscillatory structure that extends farther into the magnetic-field region $\Omega^{(h)}/\omega < 1$. In this field the spectrum branches are quite far apart and are not intermixed, as attested by the regular interference structure due to the long-wave excitations.

The interference structure vanishes when the end point of the spectrum $\Omega^{(h)}/\omega = 1.502$; $kR^{(h)} = 1.38$ is approached (Fig. 3). This singularity is distinctly observed also at other magnetic-field orientations. Figure 6, for example, shows the experimental dependence of the surface impedance of bismuth on the magnetic field $\mathbf{H}\|C_2$ ($\mathbf{k}\|C_3$, $\mathbf{H}\perp\mathbf{E}$) in the region of the first hole resonance. Equation (8) was solved using for the conductivity-tensor components general formulas of type (5) with summation of first ten cyclotron-resonance harmonics of all types of carrier ($n_{max}^{a,b,c,h} = 10$). The turning point corresponds to a narrow minimum in a magnetic field $\Omega^{(h)}/\omega = 0.723$.

We consider now the regions of the first and second resonances of light electrons at $\mathbf{H}\|C_2$. The curve in Fig. 7 was obtained for a high-frequency current perpendicular to the magnetic field, so that an extraordinary cyclotron wave with $\mathbf{E}\perp\mathbf{H}$ was excited in the sample. The figure shows also the spectrum of this wave, obtained numerically for the region $0 \leqslant kR^{(b)} \leqslant 10$, $0.7 \leqslant \omega/\Omega^{(b)} \leqslant 2$.

The following procedure was used to calculate the spectrum. To solve Eq. (8), the elements of the conductivity tensor in the interval $0 \leqslant kR^{(b)} \leqslant 2$ were calculated using general formulas of type (5), with the first 15 terms ($n_{max}^{(b)} n_{max}^{(c)} = 15$) included in the sum over n for $\sigma_{ik}^{(b)}$ and $\sigma_{ik}^{(c)}$, and the first ten ($n_{max} = 10$) for $\sigma_{ik}^{(h)}$ and $\sigma_{ik}^{(a)}$. The

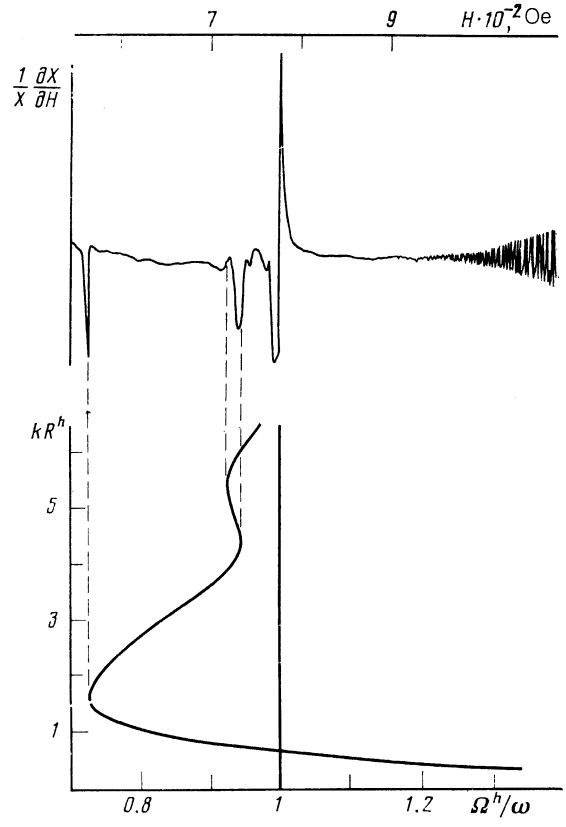

FIG. 6. Comparison of the locations of the experimentally observed singularities (upper plot) and of the end points of the spectrum of the extraordinary cyclotron wave (lower curves); $\mathbf{H}\|C_2$, $\mathbf{k}\|C_3$, $\mathbf{E}\perp\mathbf{H}$, frequency 10.22 GHz, $T = 0.35$K. The frequent oscillations near $H \gtrsim 900$ Oe are due to excitation of standing waves. The oscilations produced in the region of the cyclotron resonance are suppressed by the relatively large magnetic-field modulation amplitude.

Bessel functions and their integrals were calculated accurate to 10^{-3}. The value of $\sigma_{ik}^{(a)}$ obtained in this manner for $kR^{(b)} = 2$ agreed to within several percent of $\omega/\Omega^{(b)}$ with that calculated by expanding $\sigma_{ik}^{(a)}$ in powers of $(1/kR) - 1$ and

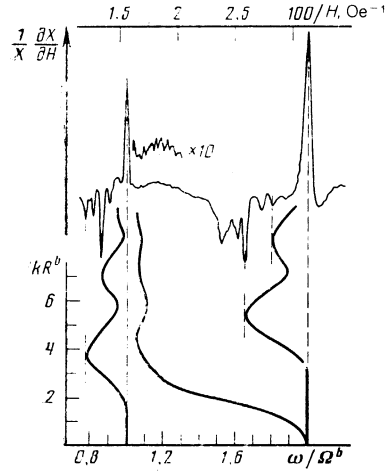

FIG. 7. Top—surface impedance of bismuth vs the reciprocal magnetic field; bottom—spectrum of extraordinary cyclotron wave as $\omega\tau \to \infty$; $\mathbf{H}\|C_2$, $\mathbf{k}\|C_3$, $\mathbf{E}\perp\mathbf{H}$, frequency 18.8 GHz, $T = 0.65$ K.

retaining the quadratic terms of this series. Asymptotic expressions for the conductivity tensor in the short-wave limit were therefore used, with $kR^{(b)} > 2$ for the a-electrons, then with $kR^{(b)} > 3.5$ for the holes, and finally with $kR^{(b)} > 5.6$ for the b- and c-electrons. It follows from a comparison of Fig. 8 (below) and Fig. 1 that the branches approaching the cyclotron-resonance lines from the direction of stronger magnetic fields are well described by Eq. (11) at $kR^{(b)} > 4.5$ and correspond to a transverse wave. The branch located near the first resonance on the weak-field side is longitudinal (10).

It can be seen from Fig. 7, where the resonances are assumed to be located at the maxima of the derivative $\partial X/\partial H$, the turning points of the extraordinary-wave spectrum correspond to the minima with the largest amplitudes. It should be noted that, just as for holes, the minima corresponding to the spectrum boundaries on the strong-field side are opposite in sign to the singularity exactly at the resonance; this is an additional argument in favor of this inter-

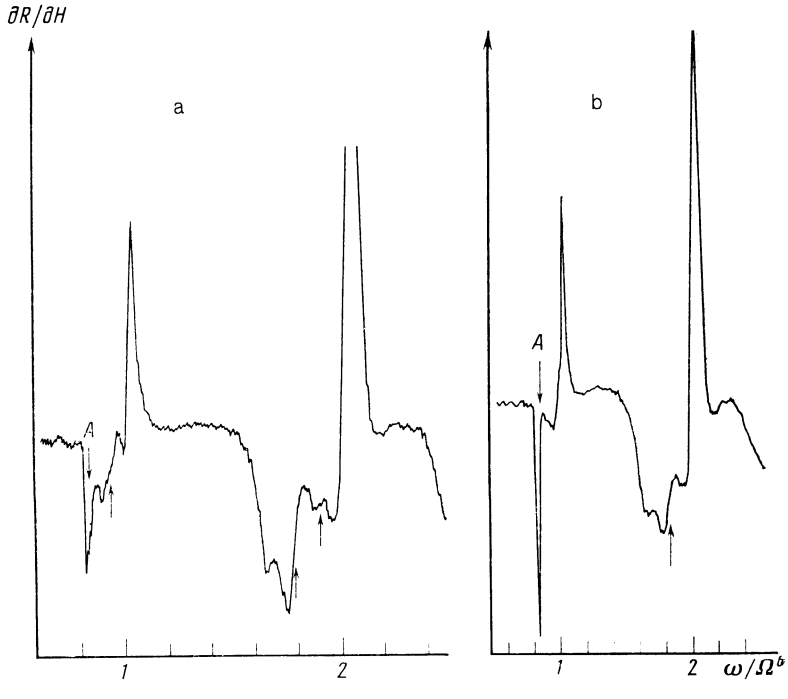

FIG. 8. The same as Fig. 7, at 31 GHz and 0.65 K (a) and at 52 GHz and 1.2 K (b). Arrows — calculated locations, marked by arrows in Fig. 1, of the singular points in the wave spectrum.

pretation. A few "extra" singularities, however, are also present. This additional structure may possibly be of the same origin as the additional peaks observed in potassium[11] and attributed to a multiply valued dispersion curve whose ambiguities lead to beats between waves having different k. Incidentally, we regard such an explanation as somewhat artificial, since we are dealing with traveling waves that damp-out in the interior of the sample, so that their interference should seemingly not influence the impedance. Moreover, in the case of hole resonance this interference should be directly manifested in the standing-wave amplitudes, something not observed in experiment (see Fig. 5). At any rate, final conclusions on this subject cannot be drawn from mere knowledge of the wave spectrum, but call for an impedance calculation, which we have not performed.

Figure 7 shows also in the interval $1.12 \leqslant \omega/\Omega^{(b)} \leqslant 1.28$ very weak oscillations due to excitation of cyclotron waves and resonances of high a-electron numbers. The corresponding resonances with numbers $n \approx 10$ were directly observed, with somewhat larger amplitude, at $\Omega^{(b)}/\omega \lesssim 0.8$.

Thus, turning points of the extraordinary-wave spectrum are distinctly manifested in the Bi impedance at $\mathbf{H} \| C_2$, $\mathbf{k} \| C_3$. As already noted, given the carrier dispersion laws (2) and (3), the positions of the end points of the spectrum, in ω/Ω coordinates, depend on the frequency of the electromagnetic wave incident on the sample. Therefore a natural check on the validity of the proposed interpretation of the observed singularities is provided by experiments performed at different frequencies.

Figures 8a and 8b show the parameters of the experimental plots of bismuth surface impedance at the respective frequencies $f_2 = 31$ GHz and $f_3 = 52$ GHz. Since the experimental setup was such that at these frequencies the current head components both along and across the field $\mathbf{H}$, special points are expected to appear on the spectra of the ordinary as well as extraordinary waves. Indeed, a dielectric anomaly of the ordinary wave (arrow A) can be seen on Fig. 8 at $\omega/\Omega^{(b)} = 0.84$. At larger $kR^{(b)}$ the dispersion curve of this wave rapidly approaches the cyclotron-resonance line. The remaining arrows, which correspond to those of Fig. 1, indicate the positions of the turning points of the extraordinary-wave spectrum, if the cyclotron-resonance field is taken to be at the zero of the derivative dR/dH; this choice agrees with the known value of the electron effective mass and meets the condition that the cyclotron resonance be periodic in the reciprocal magnetic field.

Note that with increasing frequency the fine structure becomes sparser and its resolution worse, owing to the shorter relaxation time and to multiparticle effects.[18] The plots in Fig. 8 are in a certain sense idealized: under the natural assumption that the Mathiessen rule is satisified, scattering by residual defects no longer contributes in practice to the total relaxation time, and better resolution is no longer attainable.

Thus, there are many arguments that indicate that the impedance singularities correspond to singular points in the spectrum of the cyclotron waves. The additional anomalies noted above in the case of electron resonances, however, call for additional discussion. The first to which attention must be paid is an attempt to assess the role of the deviation of the electron spectrum from quadratic. A consistent allowance for this deviation should somehow be manifested in the wave spectrum; one can expect, in particular, somewhat larger regions in which waves can exist near resonances, since the mass at a turning points is $\sim 10\%$ larger than on the central sections. It is certainly impossible, however, to shift the spectrum boundary from the value $\omega/\Omega^{(b)} = 1.66$ to 1.53 at 18.8 GHz (se Fig. 7), for it must then be assumed that effective mass is increased by 10% not just in a small vicinity of the limiting point, but on the entire Fermi surface. As seen from Fig. 8, at high frequencies even this assumption does not resolve the dilemma.

The problem of the nature of the additional minima thus remains open. A solution may be sought by assuming that the impedance receives contributions not only from electrons moving in the bulk of the metal, but also from those interacting with the boundary. In this respect, however, the electrons and holes in bismuth differ radically — the holes are scattered by the surface diffusely, and the electrons specularly.[20] The latter means, in particular, the existence of subsurface electron states whose spectrum differs from those in the bulk.[21] It is possible that this radical difference is reflected by the exact agreement of the calculated and measured impedance singularities near hole resonances, as against the more complex structure near electron resonances.

The authors thank A. S. Borovik-Romanov and M. S. Khaĭkin for their interest in the work, S. M.Cheremisin for taking part in the experiments, and V. F. Gantmakher and G. I. Leviev for a discussion of the results.

[1)] The angle between the crystallographic axis C_1 and the 1 axis, or between the crystallographic C_3 and 3, is $6^0 23'$; the binary axis C_2 is parallel to the 2 axis.

[2)] Depending on the direction of the electric field of the wave, the singularities $k = 0$ were called in Ref. 6 either the dielectric anomaly ($\mathbf{E} \perp \mathbf{H}$) or tilted-orbit resonance ($\mathbf{E} \| \mathbf{H}$). We shall use only the first name (for any polarization of the alternating field).

[1]V. D. Édel'man, Usp. Fiz. Nauk 102, 55 (1970) [Sov. Phys. Nauk **13**, 563 (1971).
[2]V. S. Édel'man, *ibid.* **123**, 257 (1977) [**20**, 819 (1977)].
[3]W. M. Walsh and P. M. Platsman, Phys. Rev. Lett. **15**, 784 (1965)
[4]É. A. Kaner and V. G. Skobov, Fiz. Tverd. Tela (Leningrad) **6**, 1104 (1964) [Sov. Phys. Solid State **6**, 851 (1964)].
[5]E.-Ni Foo, Phys. Rev. **182**, 674 (1969).
[6]G. E. Smith, L. C. Hebel, and S. J. Buchsbaum, *ibid.* **129**, 154 (1963).
[7]M. R. Trunin, Zh. Eksp. Teor. Fiz. **88**, 1834 (1985) [Sov. Phys. JETP 61, 1087 (1985)].
[8]J. Nakahara, H. Kawamuru, and Y. Sawada, Phys. Rev. **B3**, 3155 (1971).
[9]C. Guthmann, J. P. D'Haenens, and A. Libchaber, Phys. Rev. **B4**, 1538 (1971).
[10]V. P. Nabrezhnikh, D. E. Zherebchevskiĭ, and V. L. Mel'niok, Zh. Eksp. Teor. Fiz. **63**, 169 (1972) [Sov. Phys. JETP **36**, 89 (1973)].
[11]P. M. Platzmann and P. A. Wolff, *Waves and Interactions in Solid State Plasmas*, Academic, 1973.
[12]V. S. Édel'man and M. S. Khaĭkin, Zh. Eksp. Teor. Fiz. **45**, 826 (1963) [Sov. Phys. JETP **18**, 566 (1964)].
[13]V. S. Édel'man, Pis'ma Zh. Eksp. Teor. Fiz. **9**, 302 (1969) [JETP Lett. **9**, 177 (1969)].
[14]V. P. Naberezhnykh, D. E. Zherebchevskiĭ, A. P. Poluyanenko *et al.*, Fiz. Nizk. Temp. **2**, 1144 (1976) [Sov. J. Low Temp. Phys. 2, 559 (1976)].
[15]J. O. Henningsen, J. Low Temp. Phys. **4**, 163 (1971).
[16]G. L. Dunifer, P. H. Smidt, and W. M. Walsh, Phys. Rev. Lett. **26**, 1553 (1971).

[17]M. S. Khaĭkin, L. A. Fal'kovskiĭ, V. S. Édel'man, and R. T. Mina, Zh. Eksp. Teor. Fiz. **45**, 1704 (1963) [Sov. Phys. JETP **18**, 1167 (1964)].
[18]M. S. Khaĭkin, S. M. Cheremisin, and V. S. Édel'man, *ibid.* **61**, 1112 (1971) [**34**, 594 (1972)].
[19]N. E. Alekseevskiĭ, Yu. P. Gaidukov, Z. S. Gribnikov *et al.*, Conduction Electrons [in Russian], Nauka, 1985, Chap. VI.
[20]N. E. Alekseevskiĭ, Yu. P. Gaĭdukov, Z. S. Gribnikov *et al.*, *ibid.* Chaps. VIII and X.
[21]S. S. Murzin and V. T. Dolgopolov, Pis'ma Zh. Eksp. Teor. Fiz. **37**, 584 (1983) [JETP Lett. **37**, 696 (1983)].

Translated by J. G. Adashko